

Androgen receptor modulates *Foxp3* expression in CD4⁺CD25⁺*Foxp3*⁺ regulatory T-cells

Magdalena Walecki^a, Florian Eisel^a, Jörg Klug^a, Nelli Baal^b, Agnieszka Paradowska-Dogan^c, Eva Wahle^a, Holger Hackstein^b, Andreas Meinhardt^a, and Monika Fijak^a

^aDepartment of Anatomy and Cell Biology, ^bInstitute for Clinical Immunology and Transfusion Medicine, and

^cDepartment of Urology, Pediatric Urology and Andrology, Justus-Liebig-University of Giessen, 35392 Giessen, Germany

ABSTRACT CD4⁺CD25⁺*Foxp3*⁺ regulatory T (Treg) cells are able to inhibit proliferation and cytokine production in effector T-cells and play a major role in immune responses and prevention of autoimmune disease. A master regulator of Treg cell development and function is the transcription factor *Foxp3*. Several cytokines, such as TGF- β and IL-2, are known to regulate *Foxp3* expression as well as methylation of the *Foxp3* locus. We demonstrated previously that testosterone treatment induces a strong increase in the Treg cell population both in vivo and in vitro. Therefore we sought to investigate the direct effect of androgens on expression and regulation of *Foxp3*. We show a significant androgen-dependent increase of *Foxp3* expression in human T-cells from women in the ovulatory phase of the menstrual cycle but not from men and identify a functional androgen response element within the *Foxp3* locus. Binding of androgen receptor leads to changes in the acetylation status of histone H4, whereas methylation of defined CpG regions in the *Foxp3* gene is unaffected. Our results provide novel evidence for a modulatory role of androgens in the differentiation of Treg cells.

Monitoring Editor

William P. Tansey
Vanderbilt University

Received: Aug 27, 2014

Revised: Apr 27, 2015

Accepted: Jun 1, 2015

INTRODUCTION

CD4⁺CD25⁺*Foxp3*⁺ regulatory T (Treg) cells inhibit proliferation and cytokine production in effector T-cells and play a major role in immune responses and prevention of autoimmune diseases. Treg cells are potent suppressors of the proliferation of CD4⁺CD25⁻ and CD8⁺ T-cells (Thornton and Shevach, 1998; Piccirillo and Shevach, 2001), besides other immune cells, and thus control immune responses, immune homeostasis, and ultimately tolerance. Consequently these cells are used and targeted for the treatment of autoimmune and

rheumatic diseases to inhibit uncontrolled proliferation of T-cells and cytokine production (Sakaguchi *et al.*, 2008; Rudensky, 2011). A master regulator of the function of Treg cells is the transcription factor forkhead box P3 (*Foxp3*; Hori *et al.*, 2003). It is a unique marker and is stably and constitutively expressed in peripheral natural Treg cells (nTregs) arising from the thymus (Hori *et al.*, 2003). Reports have shown that peripheral naive CD4⁺CD25⁻*Foxp3*⁻ T-cells can differentiate into induced Treg cells (iTregs) after stimulation and induction of *Foxp3* (Chen *et al.*, 2003; Fontenot *et al.*, 2005). iTreg cells mediate the same suppressor activity and function as naturally occurring Treg cells. Numerous factors that are binding to the *Foxp3* locus and regulate *Foxp3* expression have been identified. The *Foxp3* promoter and three important intronic enhancers 1–3 called conserved noncoding sequences (CNSs) are known binding sites for a number of transcription factors leading to Treg-cell generation (Tone *et al.*, 2008). A further level of control is provided by epigenetic modification. Chromatin remodeling (histone acetylation and methylation), methylation of CpG clusters, and chromatin conformational changes within the *Foxp3* gene are important epigenetic mechanisms for its activation and regulation (Tone *et al.*, 2008; Okura *et al.*, 2013). CpGs within CNS2 of *Foxp3* are demethylated in Treg cells but highly methylated in *Foxp3*-negative peripheral T-cells (Kim and Leonard, 2007; Lal and Bromberg, 2009). The transcription factors Smad3 and NFAT cooperate to induce the differentiation of CD4⁺CD25⁺ Treg cells by binding to CNS2. Both factors are able to

This article was published online ahead of print in MBcC in Press (<http://www.molbiolcell.org/cgi/doi/10.1091/mbc.E14-08-1323>) on June 10, 2015.

The authors have no conflicts of interest.

Address correspondence to: Monika Fijak (monika.fijak@anatomie.med.uni-giessen.de).

Abbreviations used: acH4, acetylated histone 4; AR, androgen receptor; ARE, androgen response element; Chip, chromatin immunoprecipitation; CNS, conserved noncoding sequence; COBRA, combined bisulfite restriction assay; DHT, dihydrotestosterone; *Foxp3*, forkhead box P3; HEK-293, human embryonic kidney-293 cells; H3K27, histone 3 lysine 27; IL-2, interleukin-2; LUC, luciferase; NFAT, nuclear factor of activated T-cells; Nr4a2, nuclear receptor 4a2; P, promoter; Smad3, TGF- β , transforming growth factor β ; Treg, regulatory T-cell.

© 2015 Walecki *et al.* This article is distributed by The American Society for Cell Biology under license from the author(s). Two months after publication it is available to the public under an Attribution–Noncommercial–Share Alike 3.0 Unported Creative Commons License (<http://creativecommons.org/licenses/by-nc-sa/3.0>).

“ASCB®,” “The American Society for Cell Biology®,” and “Molecular Biology of the Cell®” are registered trademarks of The American Society for Cell Biology.

activate histone acetylation, leading to activation of the *Foxp3* promoter (Tone *et al.*, 2008). Sekiya *et al.* (2011) identified the nuclear orphan receptor Nr4a2 as a new transcription factor that binds to the *Foxp3* promoter and CNS1 enhancer. Nr4a2 activates *Foxp3* expression and mediates histone modifications within the *Foxp3* locus, whereas CpG methylation of the DNA is unaffected. The key regulator of CpG methylation is the transforming growth factor β (TGF- β) protein. It mediates CpG methylation in CNS2 by activating Stat5, which is important for opening up the CNS2 region (Ogawa *et al.*, 2014).

In experimental autoimmune orchitis, a model of testicular autoimmunity, supplementation of decreasing levels of testosterone in the rat led to a significant increase in the number of CD4⁺CD25⁺Foxp3⁺ regulatory T-cells in the testis and an inhibition of disease development (Fijak *et al.*, 2011). The protective role of testosterone in autoimmunity was also substantiated in several animal models in which castration increased the severity of experimental autoimmune encephalomyelitis (Bebo *et al.*, 1998) or led to a higher incidence of autoimmune diabetes (Fitzpatrick *et al.*, 1991). Moreover, many autoimmune diseases are more prevalent in women than in men, so that high androgen levels in men are regarded as protective (Klein, 2012; Oertelt-Prigione, 2012). In support, decreased levels of androgens were also reported in patients suffering from rheumatoid arthritis (Stafford *et al.*, 2000) or systemic lupus erythematosus (Hedman *et al.*, 1989). Therefore we wanted to test the hypothesis that testosterone can induce expression of *Foxp3* via direct binding of the androgen receptor (AR) to gene regulatory sequences, which could be responsible for an increase in the number of CD4⁺CD25⁺Foxp3⁺ regulatory T-cells.

In support of our hypothesis, we demonstrate that *Foxp3* expression is androgen dependent in human T-cells. Moreover, we identify a functional AR-binding site within the *Foxp3* locus and show that binding of AR leads to epigenetic changes. Our results provide novel evidence for a modulatory role of androgens in the differentiation or maintenance of Treg cells, which may play a role in a number of immune responses and prevention of some autoimmune diseases.

RESULTS

Androgens cause an expansion of the human Treg cell population in vitro

CD4⁺ T-cells were isolated from freshly drawn blood of young (20–35 yr of age, mean 30.6 \pm 1.7 yr) and older (>60 yr, mean 63.3 \pm 1.9 yr) men (Figure 1A) and of women who were in the a) follicular (days 1–12), b) ovulatory (days 12–14), and c) luteal (days 16–24) phases of their menstrual cycle (20–35 yr, mean 29.13 \pm 2.4 yr) or d) were postmenopausal (>50 yr, mean 55.17 \pm 1.5 yr; Figure 1B). Cells were subsequently stimulated with different doses of dihydrotestosterone (DHT; 0–500 nM) for 48 h. Stimulation of T-cells during the follicular and luteal phases did not show any significant influence on *Foxp3* expression as compared with vehicle controls or freshly isolated cells (0 h = directly after isolation; Figure 1B). Of note, the number of CD4⁺CD25⁺Foxp3⁺ Treg cells was significantly increased when CD4⁺ T-cells collected in the ovulatory phase were stimulated with 10 or 100 nM DHT (Figure 1B, b). Maximal effects were observed with 10 and 100 nM DHT, whereas 500 nM DHT was ineffective. Representative flow cytometry plots are shown in Figure 1C. In contrast, stimulation of T-cells isolated from older postmenopausal women (>50 yr) as well as from younger (20–35 yr, mean 30.6 \pm 1.7 yr) and older (>60 yr, mean 63.3 \pm 1.9 yr) men revealed no significant increase of the CD4⁺CD25⁺Foxp3⁺ T-cell population after stimulation with DHT at the indicated doses, although a slight increase in the cohort of older women was noted at higher doses (Figure 1, A

and C). A direct comparison of *Foxp3* expression in CD4⁺CD25⁺ T-cells between all investigated blood donor groups directly after isolation ($t = 0$ h; Figure 1D) showed a significantly higher number of Treg cells in T-lymphocytes isolated from women in the ovulatory phase than in postmenopausal women and men.

The number of CD4⁺CD25⁺Foxp3⁺ Treg cells is higher in women than in men

On the basis of the gender-specific response of *Foxp3* protein levels in T-cells following stimulation with DHT, we analyzed the CD4⁺CD25⁺Foxp3⁺ T-cell population in fresh blood of women and men. Isolated peripheral blood mononuclear cells (PBMCs) from young women (19–35 yr) and men (23–35 yr) were stained for Treg-cell markers and analyzed by flow cytometry. PBMCs revealed a significantly higher percentage of CD4⁺CD25⁺Foxp3⁺ Treg cells in the population of CD4⁺CD25⁺ T-cells in women (63 \pm 3%) than in men (50 \pm 3%). Numbers of CD4⁺CD25⁺ T-cells in investigated subjects did not differ significantly and are gender independent (women 2.4 \pm 0.2% vs. men 2.0 \pm 0.2%; Table 1). Similarly, comparison of T-cell populations in older women (>50 yr) and men (>60 yr) showed a significantly higher percentage of CD4⁺CD25⁺Foxp3⁺ Treg cells and CD4⁺CD25⁺ T-cells in female than in male PBMCs (Table 1). Furthermore, relative expression levels of AR and *Foxp3* mRNAs were analyzed in different immune cell populations across genders (CD4⁻, CD4⁺CD25⁻ [T-cells] and CD4⁺CD25⁺CD127^{dim/-} [Treg cells]). *Foxp3* and AR mRNA expression was detectable in all investigated cell populations; however, the quantitative real-time PCR (qRT-PCR) results revealed no significant changes in Treg cells from both genders (Figure 1, E and F).

In human embryonic kidney-293 cells, AR is androgen dependently recruited to an intronic region of the *Foxp3* gene

The *Foxp3* gene is characterized by a promoter (P) and two enhancer elements (CNS1 and 2) located in the intron between non-coding exons -2b and -1 (Figure 2A). To investigate its androgen-dependent regulation, we cloned luciferase reporter (LUC) constructs containing the *Foxp3* promoter and/or two fragments that included one of the two enhancer elements (fragment I or II) as indicated (Figure 2B). Cotransfection of an AR expression construct together with the luciferase reporter plasmid containing *Foxp3* enhancer fragment I and the promoter in human embryonic kidney (HEK)-293 cells (Figure 2B) resulted in a strong induction of luciferase activity ([20.3 \pm 4.5]-fold) compared with the construct that only contained the promoter ([2.9 \pm 0.4]-fold). The androgen response mediated by fragment II and the promoter was significantly lower ([6.7 \pm 0.8]-fold). Removal of the promoter caused a significant reduction in androgen-dependent luciferase activation mediated by fragment I ([4.9 \pm 0.9]-fold) or fragment II ([3.3 \pm 1.2]-fold) alone (Figure 2B). Preincubation for 1 h with the antiandrogen flutamide abrogated the androgen response mediated by the promoter alone and by enhancer fragment I or II plus promoter. We conclude from these results that the androgen response of the *Foxp3* gene is mediated by the AR binding to fragment I.

To identify functional AR-binding sites in fragment I, we performed chromatin immunoprecipitation (ChIP) assays with HEK-293 cells (Figure 2, D and E) cotransfected with the AR expression construct and the promoter or fragment I construct of the *Foxp3* gene. After ChIP with an anti-AR antibody, the coprecipitation of two promoter regions (A and B) for comparison purposes and five regions from fragment I (C–G; see schematic scheme in Figure 2C) was analyzed by qRT-PCR (Figure 2D). Fragment I regions C–G, and in particular

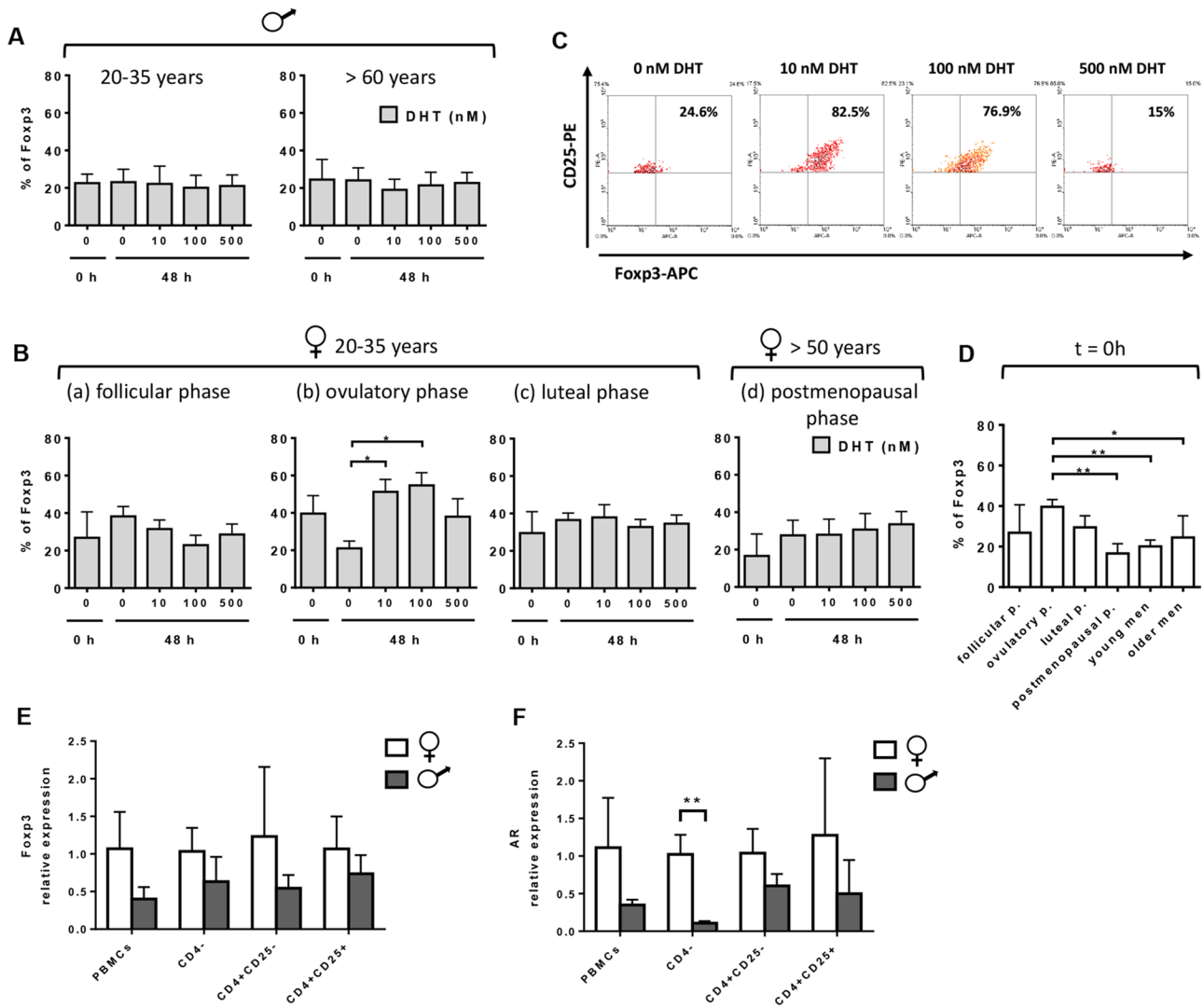


FIGURE 1: Gender differences in androgen-dependent expansion of the Fopx3⁺ Treg cell population. DHT dependence of Fopx3 expression in human Treg cells (CD4⁺CD25⁺Fopx3⁺) from peripheral blood T-cells in men (A) and women (B) in vitro. Isolated peripheral T-cells were incubated with 0–500 nM DHT for 48 h at 37°C or analyzed directly after isolation (time point 0 h). Data were obtained from (A) 20- to 35-yr-old (*n* = 9) and >60-yr-old (*n* = 6) men and (B) 20- to 35-yr-old women in the follicular (*n* = 5), ovulatory (*n* = 9), and luteal phase (*n* = 5) and >50-yr-old women (*n* = 6). Percentage of CD4⁺CD25⁺Fopx3⁺ Treg cells within the population of CD4⁺CD25⁺ T-cells measured by flow cytometry. (C) Representative flow cytometry plots evaluated in B. T-cells were stained with CD4-FITC, CD25-PE, and Fopx3-APC. Numbers represent the percentage of Treg cells in the gated CD4⁺CD25⁺ population. (D) Comparison of Fopx3 expression in CD4⁺CD25⁺ T-cells between all groups from A and B directly after isolation (*t* = 0 h). (E, F) Comparison of Fopx3 (E) and AR (F) mRNA expression in PBMCs and CD4⁻, CD4⁺CD25⁻, and CD4⁺CD25⁺CD127^{dim/-} T-cells from peripheral blood of three men and women by qRT-PCR. mRNA expression levels of Fopx3 and AR in PBMCs, CD4⁻, CD4⁺CD25⁻, and CD4⁺CD25⁺CD127^{dim/-} T-cells from men were normalized to the Fopx3 (E) or AR (F) expression for each cell type. Data are expressed as mean ± SEM. The *p* values were determined by one-way ANOVA multiple comparison (B) or nonpaired Student's *t* test (D, F). **p* < 0.05, ***p* < 0.01.

region F, were significantly coprecipitated with the anti-AR antibody compared with immunoglobulin G (IgG 17 ± 3% of input for region F; Figure 2D). Moreover, a comparison between DHT-treated (+DHT) and nontreated (-DHT) samples reveals a statistically significant hormone-dependent recruitment of AR to regions C–G in transfected HEK-293 cells that is particularly prominent in region F (Figure 2E).

AR binds to an element in the Fopx3 gene that is located in region F or its vicinity

For the analysis of androgen response elements (AREs) within the Fopx3 gene, a number of deletion constructs and mutants were gen-

erated (Figure 3, A and C) and transfected into HEK-293 cells. ChIP/qRT-PCR experiments using regions C–G as detailed before (Figure 2) revealed that deletion of 314 base pairs at the 5' end (Δ314) had no influence on the coimmunoprecipitation of AR and regions C–G as compared with the full-length construct (FL) (Figure 3B). After deletion of another 209 base pairs (Δ523), which included region C, immunoprecipitation of AR led to a statistically significant decrease in coprecipitation of regions E–G. Truncation of 698 base pairs (Δ698) led to a further decrease in coprecipitation of only region F. Conversely, when the construct with deleted region F (FL ΔF) was transfected, coimmunoprecipitation of region C was not significantly affected (Figure 3B).

	Men 23–35 yr (n = 6)	Women 19–35 yr (n = 7)	p	Men >60 yr (n = 6)	Women >50 yr (n = 6)	p
Percentage of CD4 ⁺ CD25 ⁺ in PBMCs	2.0 ± 0.20	2.4 ± 0.18	n.s.	2.5 ± 0.39	4.3 ± 0.52	0.02
Percentage of CD4 ⁺ CD25 ⁺ Foxp3 ⁺ within CD4 ⁺ CD25 ⁺ population	50 ± 3.12	63.2 ± 3.33	0.015	41.38 ± 4.4	59.4 ± 5	0.02
Percentage of CD4 ⁺ CD25 ⁺ Foxp3 ⁺ within PBMCs	0.91 ± 0.19	1.5 ± 0.1	0.017	1.08 ± 0.24	3.95 ± 0.9	0.02

The p values were determined by nonpaired t test (*p < 0.05).

TABLE 1: Percentage of CD4⁺CD25⁺ and CD4⁺CD25⁺Foxp3⁺ T-cells within the PBMC population isolated from human male and female peripheral blood.

To identify AREs, bioinformatic analyses identified several putative AREs in the *Foxp3* gene, including one element each in regions C, D, and F (Figure 3C). These three putative AREs were mutated and again tested in ChIP/qRT-PCR experiments (Figure 3D). Compared to the wild type, mutation of either ARE C or ARE F, but not ARE D, significantly prevented coprecipitation of DNA fragments containing region F, whereas all mutants did not affect coprecipitation of region C. Therefore these results indicate that in HEK-293 cells, AR is binding to an element in the *Foxp3* gene that is located in region F, whereas a factor binding to an element in region C aids in binding of AR to region F.

In Treg cells, but not in non-Treg cells, AR is hormone dependently recruited to region F of the *Foxp3* gene

Recruitment of AR to the *Foxp3* gene was also quantified in primary human Treg cells (CD4⁺CD25⁺CD127^{dim/-}) and in non-Treg cells (CD4⁺CD25⁻) isolated from peripheral blood of young (mean 26.3 ± 0.8 yr, n = 5) and older (mean 49.7 ± 1.3 yr, n = 4) female (Figure 4, A and B) and young (mean 30.2 ± 2 yr, n = 5) and older (mean 47 ± 0.5 yr, n = 3) male (Figure 4, D and E) donors treated or not with DHT (Figure 4).

As in HEK-293 cells, binding of AR was observed to region F but not to the *Foxp3* promoter (regions A and B) or fragment II (regions H–K) in Treg cells of young women and men (Figure 4, A and D) treated with DHT. No binding of AR to the *Foxp3* gene was observed in ChIP assays performed with Treg cells from older female and male blood donors (Figure 4, A and D) or non-Treg cells (Figure 4, B and E). Of note, AR recruitment in Treg cells isolated from women was stronger than in cells from men.

Hormone dependence of AR binding was demonstrated by comparing Treg cells isolated from young female and male blood donors that were treated with DHT with untreated cells (Figure 4, C and F). ChIP experiments revealed that significant coprecipitation of AR and region F occurred only in the presence of DHT, whereas recruitment of AR to fragment C was weak and hormone independent.

The *Foxp3* locus is epigenetically modified after androgen treatment

Changes in the acetylation and methylation status of chromatin are an established mechanism in the regulation of *Foxp3* gene expression (Tone et al., 2008; Sekiya et al., 2011). To find out whether acetylation of histone H4 (acH4) could also play a role in mediating the observed androgen response, we performed an in vitro pilot experiment in HEK-293 cells before we investigated primary T-cells (Figure 5, A and B). HEK-293 cells were cotransfected with a *Foxp3* fragment I (+277 to +2275) containing construct together with an AR expression plasmid and treated (+DHT) or not (-DHT) with

DHT. Using an anti-acH4 antibody, coprecipitation of DNA fragments containing regions C–F strongly increased after stimulation with DHT (Figure 5B). This indicated also that chromatin reconstitution occurred to some extent within the *Foxp3* gene on the transfected construct. Next epigenetic changes were analyzed in primary Treg cells (CD4⁺CD25⁺CD127^{dim/-}) and non-Treg cells (CD4⁺CD25⁻) that were freshly isolated from buffy coats of young women (mean age 25.5 ± 0.9 yr) and men (mean age 29.6 ± 1.5 yr) and subsequently stimulated with and without DHT. DHT treatment resulted in a significant increase in acH4 in region F of the *Foxp3* gene in Treg cells from women (Figure 5, C–F). In contrast, treatment of male Treg and non-Treg cells with DHT did not change the acetylation status of the two investigated regions, C and F (Figure 5, G–J).

Besides modifications characteristic of gene activation (acH4), we also investigated the repressive histone modification H3K27me3 in regions C and F (Figure 6). Independent of hormone, regions C and F were not trimethylated on H3K27 in Treg and non-Treg cells of women or men (Figure 6). All ChIP/qRT-PCR results for region F obtained in Treg and non-Treg cells from women and men are summarized in Table 2.

DHT treatment does not change CpG methylation within the *Foxp3* gene

Previous studies revealed that CpGs in the promoter region as well as in an intronic CpG island of the *Foxp3* gene are mostly demethylated in Treg cells and highly methylated in effector T-cells (Floess et al., 2007; Huehn et al., 2009). To investigate whether binding of AR to the *Foxp3* gene leads to differential CpG methylation, we evaluated the methylation status of several CpGs close to the mapped ARE in region F and its vicinity (Figure 7A) by pyrosequencing (Figure 7, B and C) and combined bisulfite restriction assay (COBRA; Figure 7, D and E) in CD4⁺CD25⁺ and CD4⁺CD25⁻ T-cell populations isolated from blood of women and treated or not with DHT. For all tested CpGs, a higher methylation rate was found in CD4⁺CD25⁻ T-cells than in CD4⁺CD25⁺ T-cells. However, DNA methylation rates in tested CpGs were independent of DHT treatment in both subpopulations (Figure 7E). Data clustering to increase the sensitivity of analysis for each individual investigated also demonstrated no significant DHT-dependent change in the methylation status of *Foxp3* in both T-cell populations (Figure 7F).

DISCUSSION

Expression of AR and its signaling pathways has been reported in immune cells such as neutrophils, macrophages, and B- and T-cells (Viselli et al., 1997; Mantalaris et al., 2001) but not in CD4⁺CD25⁺Foxp3⁺ Treg cells. However, data from our previous

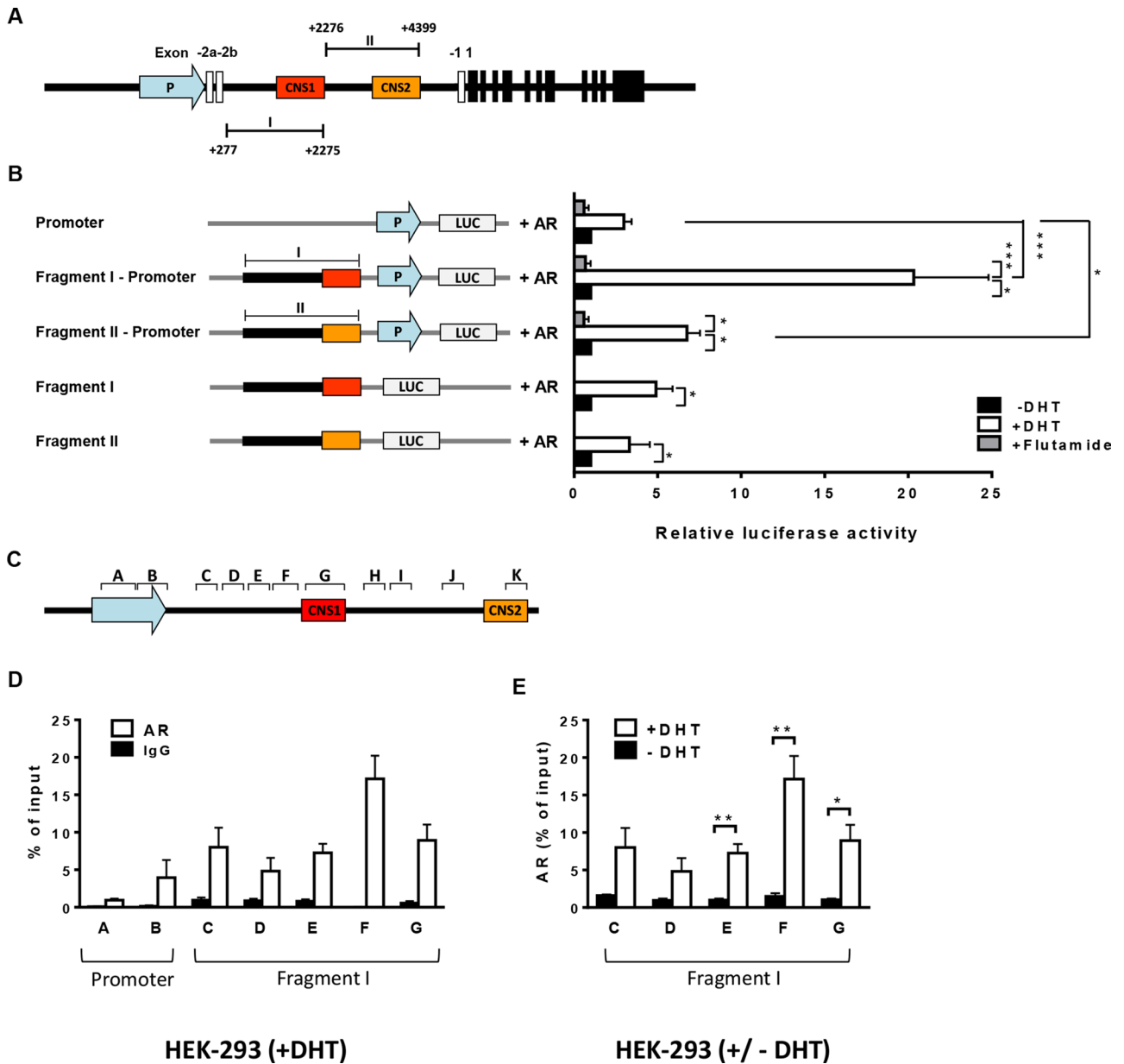


FIGURE 2: The *Foxp3* gene is activated by the AR in a hormone-dependent manner. (A) Schematic representation of the human *Foxp3* locus. (B) Transactivation of the *Foxp3* gene by androgens is predominantly mediated by fragment I. Transcriptional activities and AR-mediated transactivation of *Foxp3* promoter constructs were analyzed by luciferase reporter assays in HEK-293 cells. Left, schematic representation of *Foxp3* luciferase reporter constructs used. Right, HEK-293 cells were transiently cotransfected with AR expression and *Foxp3* luciferase reporter constructs and treated with vehicle (black bars; $n = 8-13$), 0.5 nM DHT (white bars; $n = 8-13$), or the antiandrogen flutamide (3 nM) followed by 0.5 nM DHT (gray bars; $n = 3$) for 16 h. pSV- β -Gal was used for performing well-to-well normalization. The activity of the negative control without DHT was always set to 1. (C) Location of amplicons within the *Foxp3* gene used for ChIP/qRT-PCR assays. Primer pairs A and B bind within the promoter, C–G within fragment I, and H–K within fragment II (A). (D, E) Analysis of AR binding to the *Foxp3* gene by ChIP/qRT-PCR assay. (D) HEK-293 cells were transiently cotransfected with AR expression and *Foxp3* promoter (for amplicons A and B only) or fragment I constructs and treated with 0.5 nM DHT for 16 h. Cell lysates were immunoprecipitated with anti-human AR antibody (white bars) or control IgG (black bars). (E) Hormone dependence was investigated by comparing AR recruitment to regions C–G in fragment I in the presence (white bars) or absence (black bars) of DHT. Data are mean \pm SEM of four (D) and nine (E) independent experiments. Coprecipitated DNA was analyzed by qRT-PCR with primer pairs A–G (Table 4). The p values were determined by one-way ANOVA accompanied by the Bonferroni test (B) or nonpaired t test (E). * $p < 0.05$, ** $p < 0.01$, *** $p < 0.001$. CNS, conserved noncoding sequence; LUC, luciferase gene; P, promoter.

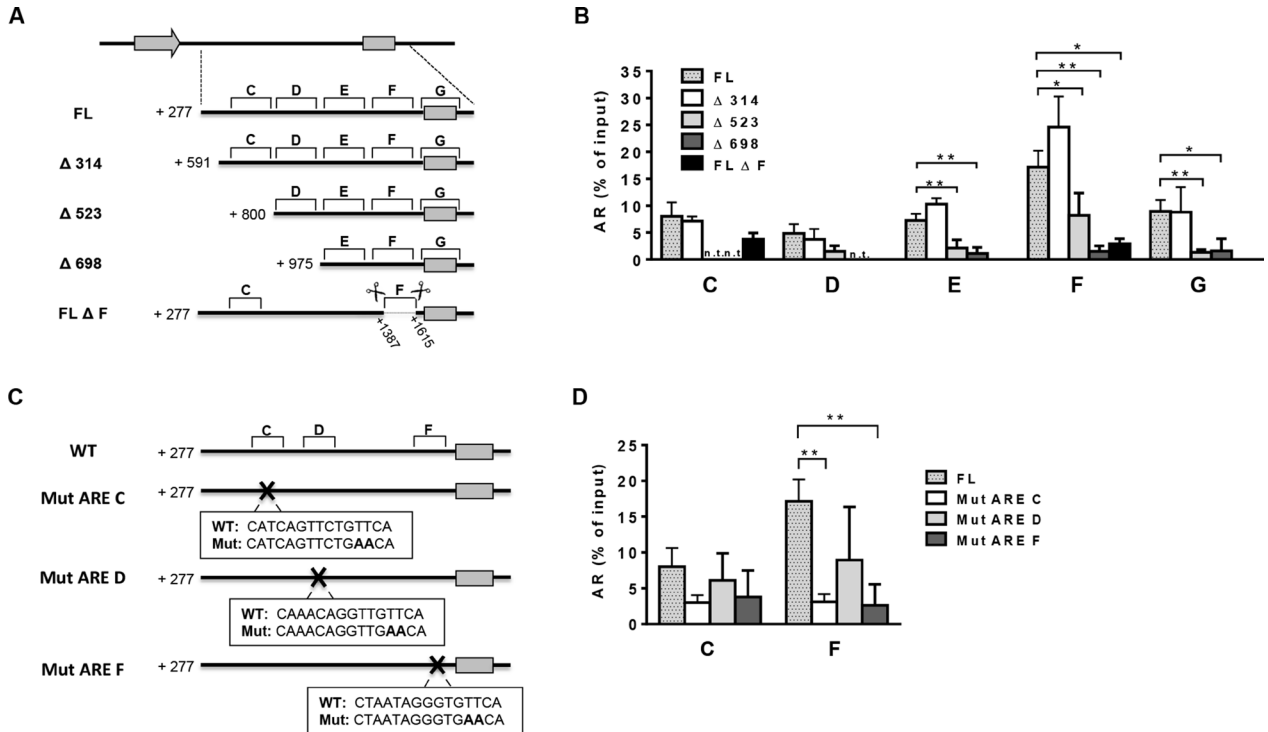


FIGURE 3: An AR-binding site is present in fragment F of the *Foxp3* gene in HEK-293 cells. (A) Schematic representation of generated deletion constructs of *Foxp3* fragment I. (B) ChIP/qRT-PCR analyses of AR binding to the deletion constructs shown in A after transfection into HEK-293 cells together with the AR expression construct and stimulation with 0.5 nM DHT for 16 h. Cell lysates were immunoprecipitated with anti-human AR antibody. (C) Schematic representation of constructs with point mutations (position in the gene indicated by x) introduced into putative AREs of *Foxp3* fragment I. (D) ChIP/qRT-PCR analyses of AR binding to constructs with point mutations after transfection into HEK-293 cells together with the AR expression construct and stimulation with 0.5 nM DHT for 16 h. Cell lysates were immunoprecipitated with anti-human AR antibody. Values are presented as the percentage of corresponding input of five or six independent experiments. Coprecipitated DNA was analyzed by qRT-PCR with specific primer pairs C–G (Table 4). FL, full length; n.t., not tested; WT, wild type. The *p* values were determined using the nonpaired *t* test. **p* < 0.05, ***p* < 0.01.

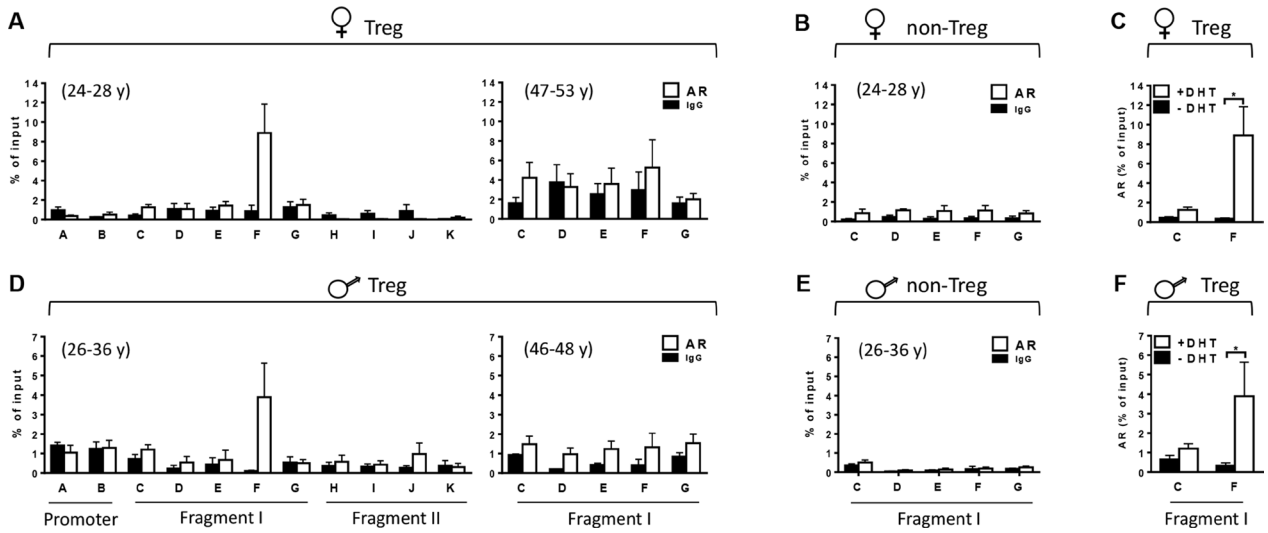


FIGURE 4: DHT induces binding of AR to region F within the *Foxp3* gene. (A, B, D, E) Analysis of AR binding to different regions (A–K) of the *Foxp3* gene by ChIP/qRT-PCR assays with isolated human Treg (CD4⁺CD25⁺; A, D) and non-Treg (B, E) cells from peripheral blood of young (mean 26.3 ± 0.8 yr, *n* = 5) and older (mean 49.7 ± 1.3 yr, *n* = 4) women and young (mean 30.2 ± 2 yr, *n* = 5) and older (mean 47 ± 0.5 yr, *n* = 3) men after stimulation with DHT for 16 h. Cell lysates were immunoprecipitated with anti-human AR antibody (white bars) or control IgG (black bars). (C, F) Comparison of +DHT (white bars) vs. –DHT (black bars) treatment on AR recruitment to regions C and F in fragment I of the *Foxp3* gene in Treg cells isolated from women (C; *n* = 5) and men (F; *n* = 5). Values are presented as the percentage of corresponding input. Coprecipitated DNA was analyzed by qRT-PCR with specific primer pairs A–K (Table 4). The *p* values were determined using the nonpaired Student’s *t* test or the Wilcoxon–Mann–Whitney test, depending on the distribution of data. **p* < 0.05 was considered statistically significant.

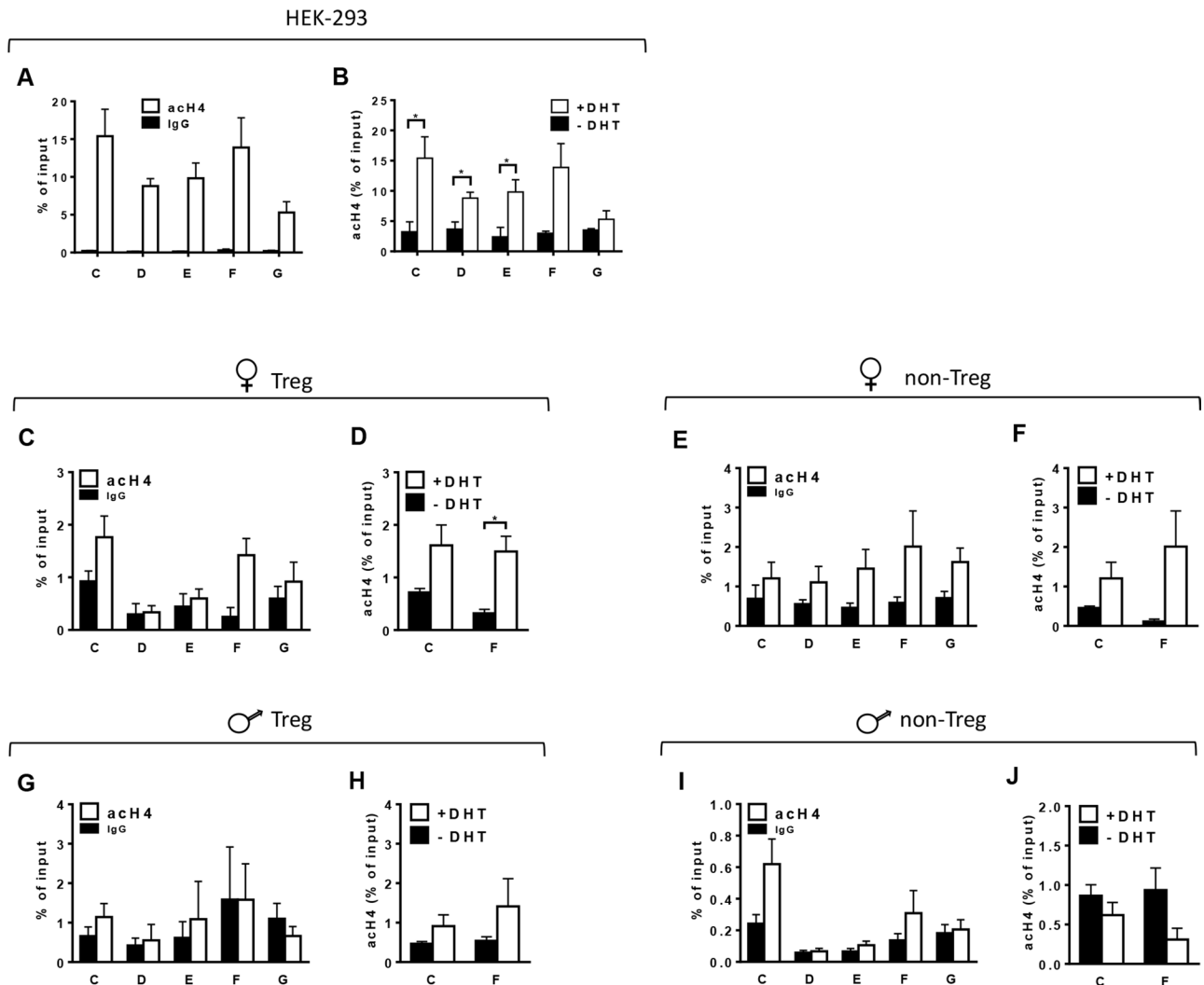


FIGURE 5: AR induces histone H4 acetylation (acH4) in *Foxp3* fragment I. (A) ChIP/qRT-PCR analyses of transfected HEK-293 cells after stimulation with 0.5 nM DHT for 16 h. Histone acetylation was assayed by using anti-acetyl histone H4 (white bars) and control IgG (black bars) antibodies for ChIP and primer pairs C–G for qRT-PCR. (B) Comparison between +DHT (white bars) and –DHT (black bars) treatment on acH4 in region C–G in fragment I of the *Foxp3* gene in HEK-293 cells. (C–J) ChIP/qRT-PCR analyses of histone acetylation in Treg (C, D, G, H) and non-Treg (E, F, I, J) cells isolated from peripheral blood of young women (mean age 25.5 ± 0.9 yr) and men (mean age 29.6 ± 1.5 yr) without and after stimulation with DHT for 16 h. (C, G, E, I) ChIP/qRT-PCR analyses of acH4 using anti-acetyl histone H4 (white bars) and control IgG (black bars) antibodies in Treg and non-Treg cells isolated from blood of women (C, E) and men (G, I) after DHT stimulation. (D, F, H, J) Direct comparison of +DHT (white bars) vs. –DHT (black bars) treatment on acH4 in regions C and F of the *Foxp3* gene in Treg (D, H) and non-Treg cells (F, J) from women (D, F) and men (H, J). Coprecipitated DNA was analyzed by qRT-PCR with specific primer pairs C–G (Table 4). The *p* values were determined using nonpaired Student's *t* test. **p* < 0.05 was considered statistically significant.

experiments indicated that androgens may act on Treg cells and expansion of this subpopulation after testosterone supplementation in rat autoimmune orchitis and testosterone-stimulated generation and functional differentiation of Treg cells from rat splenic T-cells (Fijak *et al.*, 2011). These studies pointed to a direct role of testosterone in the expansion of *Foxp3*⁺ Treg cells. By investigating human Treg and non-Treg (CD4⁺CD25⁻) cells from men and women, we provide here novel evidence in support of our hypothesis. We were able to show that the *Foxp3* gene is more responsive to androgen treatment in T-cells isolated from women than in men, indicating gender-specific androgen signaling. However, in women, the DHT stimulatory effect was visible only in the ovulatory phase of the men-

strual cycle. Of note, *Foxp3*⁺ Treg cell numbers isolated from female PBMCs are more than two times higher from day 3 to day 12 of the menstrual cycle (Arruvito *et al.*, 2007). This increase shows a strong correlation with serum estrogen, but also with testosterone levels. Although much lower than in men, testosterone peaks around ovulation, showing a sharp increase, with free testosterone levels reaching almost double the concentration than in other parts of the cycle (Goebelsmann *et al.*, 1974; Burger, 2002; Rothman *et al.*, 2011). High testosterone levels during ovulation could help to counterbalance the proinflammatory effects of the elevated estrogen levels characteristic for this phase of the menstrual cycle. Although estradiol can stimulate the conversion of CD4⁺CD25⁻ T-cells into

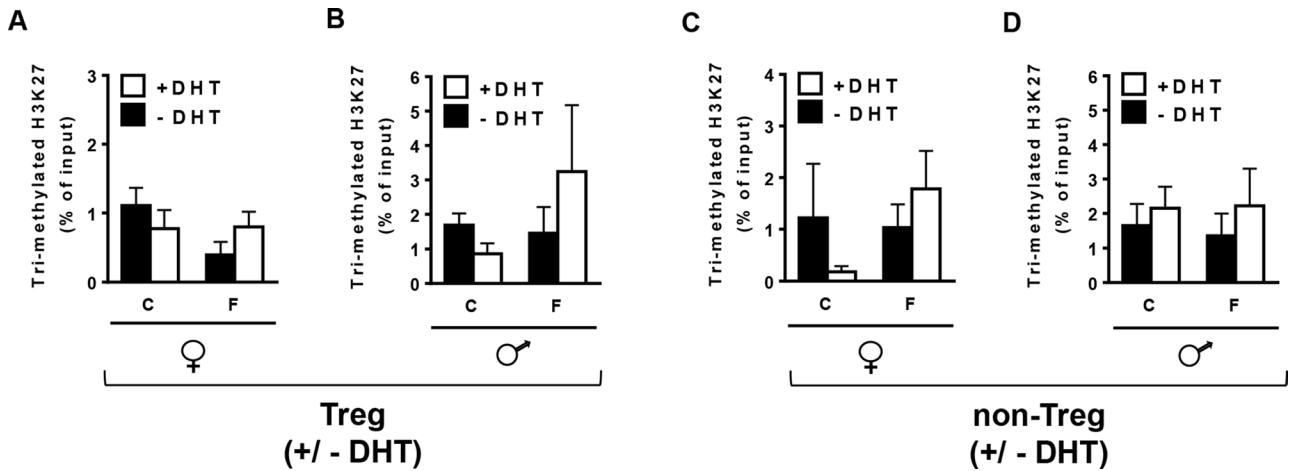


FIGURE 6: AR binding does not change histone 3 trimethylation (H3K27) status in regions C and F of *Foxp3* fragment I. (A–D) ChIP/qRT-PCR analyses of trimethylation of H3K27 using anti-H3K27me3 antibodies in Treg (A, B) and non-Treg (C, D) cells isolated from blood of women (A, C) and men (B, D) and stimulated with (white bars) or without (black bars) DHT for 16 h. Coprecipitated DNA was analyzed by qRT-PCR with specific primer pairs C and F (Table 4). All values are presented as percentage of corresponding input.

CD4⁺CD25⁺ T-cells (Tai *et al.*, 2008), progesterone has been shown to induce *Foxp3* expression and generate highly stable Treg cells under inflammatory conditions (Lee *et al.*, 2012). Therefore it is tempting to hypothesize that androgens, estrogens, and progesterone all act in synergy to ensure the contribution of the immune system to reproductive success. With testosterone high at ovulation, when also estradiol peaks, the *Foxp3*⁺ Treg subpopulation can expand as a means to prevent uncontrolled production of proinflammatory cytokines, whereas the increase of progesterone during the luteal phase establishes an environment that allows sperm to survive in the female reproductive tract. In support, increases in the number of *Foxp3* Treg cells are associated with a better pregnancy rate in natural and in vitro fertilization outcomes (Polanczyk *et al.*, 2005; Schumacher *et al.*, 2009; Zhou *et al.*, 2012). Of interest, a single injection of testosterone into female rodents causes neonatal androgenization and also increases the relative and absolute numbers of CD4⁺CD25⁺*Foxp3*⁺ Treg cells in peripheral blood (Leposavić *et al.*, 2009).

In continuation of our previous studies, we were able to show here that stimulation of Treg cells with androgens leads to binding of AR to the *Foxp3* gene and modifies the acetylation status of histones in the vicinity of the AR-binding site. Using a number of *Foxp3* gene fragments driving luciferase expression in HEK-293 cells (Figure 2), we showed that the promoter and fragments I and II individually confer a three- to fivefold androgen response. When the promoter is combined with fragment II, the contribution of both

sequences is additive, whereas promoter and fragment I act synergistically and confer a strong 20.3-fold androgen response. The androgen response appears to be mediated through classical AR signaling, because androgen-dependent gene activation of the *Foxp3* gene could be abrogated with the antiandrogen flutamide. By using ChIP experiments, we observed significant hormone-dependent recruitment of AR to fragment I centered around fragment F in HEK-293 cells (Figure 2) and exclusively to region F in CD4⁺CD25⁺CD127^{dim/-} Treg cells from young women and men (Figure 4). To identify the ARE, we transfected fragment I deletion constructs and constructs with point mutations into HEK-293 cells and measured AR recruitment by ChIP (Figure 3). Mutation of two predicted AREs in regions C and F abolished AR recruitment, whereas mutation of another predicted ARE in region D had no effect. The results indicate that there is a single ARE in region F and that recruitment of AR to region F is potentiated by region C. Region C seems not to harbor a bona fide ARE because there is no significant hormone-dependent recruitment of AR in HEK-293 cells (Figure 2E) and Treg cells of young women and men (Figure 4).

In support of our findings, Hu *et al.* (2010) mapped one AR-binding site to the mouse *Foxp3* gene in a genome-wide in vivo mapping of AR-binding sites in the mouse epididymis. Because AR is also known to interact with many other transcription factors, such as SMAD3, REL, Fos, Jun, FOXO, and Ets-1 (Tone *et al.*, 2008), that are involved in activation of the *Foxp3* promoter, it is tempting to speculate that AR bound to the ARE in region F may cooperate with some or one of these factors binding to region C in activating *Foxp3* transcription.

Gene expression requires the conversion of transcriptionally silent, condensed heterochromatin into active euchromatin. One mechanism involved in gene activation is acetylation of histone 4 (Allfrey *et al.*, 1964; Struhl, 1998; Akhtar and Becker, 2000), whereas gene silencing requires methylation of histones like trimethylation of lysine 27 of histone 3 (H3K27me3; Peters *et al.*, 2003; Vakoc *et al.*, 2005, 2006). AR can play an active role in histone modification by recruiting different coregulators or corepressors, as shown in prostate cancer (Heinlein and Chang, 2002; Chmelar *et al.*, 2007). Encouraged by these reports, we analyzed histone acetylation and methylation in region CNS1 of the *Foxp3* locus and showed that

	Treg		non-Treg	
	Women	Men	Women	Men
AR	↑	↑	⇒	⇒
acH4	↑	(⇒)	(↑)	(↓)
H3K27me3	⇒	⇒	⇒	⇒

Parentheses indicate that the change is not statistically significant.

TABLE 2: Summary of ChIP/qRT-PCR results for region F of the *Foxp3* gene in women and men.

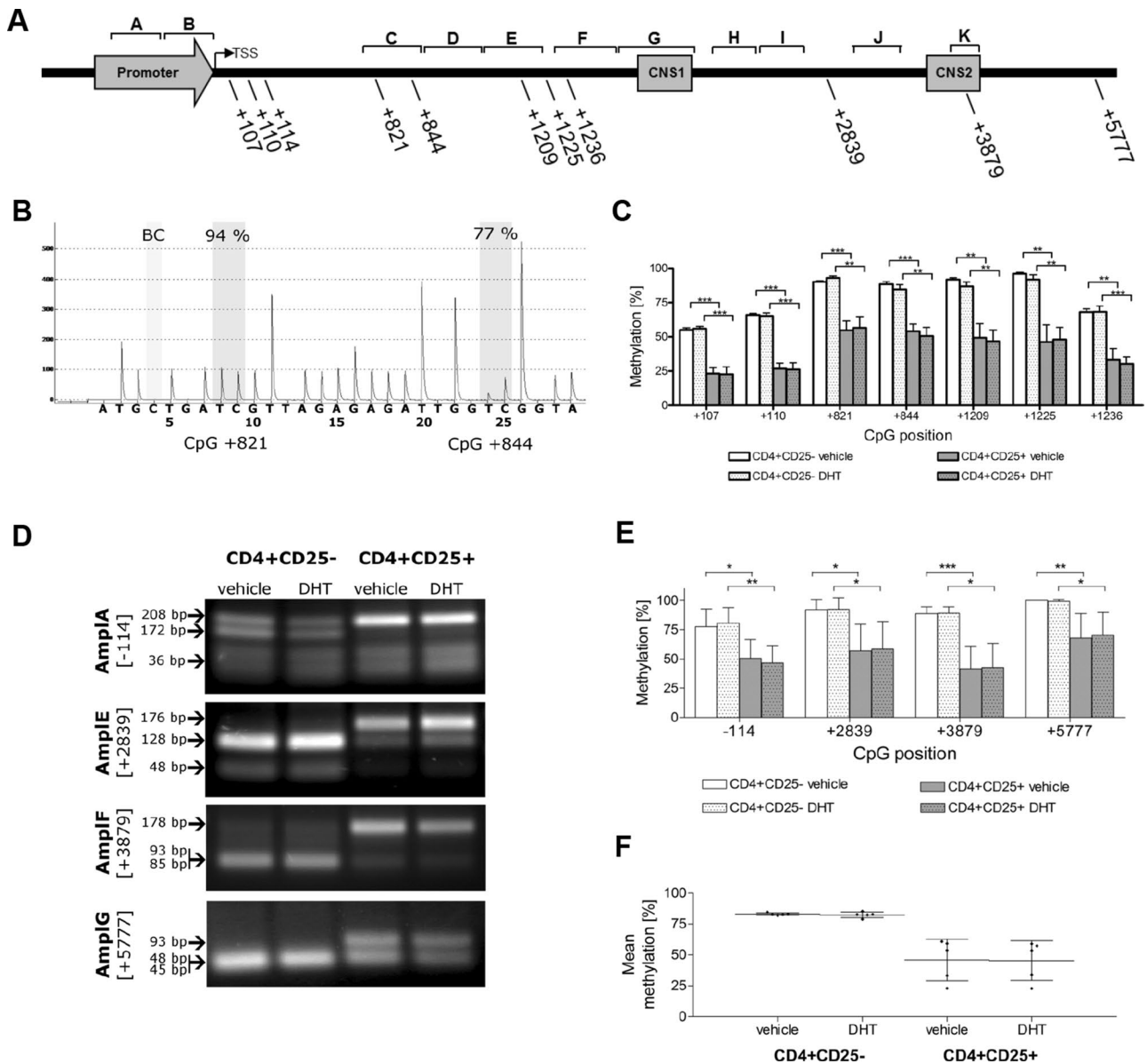


FIGURE 7: AR binding does not mediate demethylation of defined regions of CpGs within the *Foxp3* gene.

(A) Schematic representation of the localization of selected CpGs within the *Foxp3* gene. CNS, conserved noncoding sequence; TSS, transcription start site. (B) Example of pyrosequencing readout of *Foxp3* CpGs +821 and +844 in genomic DNA isolated from T-cells of women after 10 nM DHT stimulation for 15 h and subsequent bisulfite conversion. Efficiency of bisulfite conversion was demonstrated by using a bisulfite control (BC) corresponding to a non-CpG cytosine residue that, after bisulfite conversion, no longer leads to a C signal. (C) Summary of pyrosequencing analyses of defined *Foxp3* CpGs after DHT treatment in isolated CD4⁺CD25⁻ (bright bars) and CD4⁺CD25⁺ (gray bars) T-cells from peripheral blood of women. (D) COBRA was used to quantify the methylation status of four additional *Foxp3* CpGs. After bisulfite conversion, isolated genomic DNA from DHT-stimulated CD4⁺CD25⁻ and CD4⁺CD25⁺ T-cells from blood of women was purified, amplified, and cut with *TaqI* restriction enzyme. Methylation status was assessed by comparison of the signal intensities of restriction products ($n = 5$). Upper bands indicate undigested PCR products corresponding to unmethylated *TaqI* sites. Representative gel pictures from one donor are shown. (E) Summary of COBRA analyses of *Foxp3* CpGs -114, +2839, +3879, and +5777 after DHT stimulation of isolated CD4⁺CD25⁻ (bright bars) and CD4⁺CD25⁺ (gray bars) T-cells from blood of women. (F) Compendium of achieved methylation values for all defined CpG regions from B and D shown as mean methylation for each individual ($n = 5$). The p values were determined by nonpaired t test. * $p < 0.05$, ** $p < 0.01$, *** $p < 0.001$.

activation of AR by DHT led to a strong increase in acetylation of histone H4 within region F in Treg cells from women but not from men (Figure 5, D and H). In contrast, trimethylation of H3K27 was not affected in Treg and non-Treg cells of women or men (Figure 6).

Our findings suggest that DHT-liganded AR can open up the DNA for binding of additional transcription factors, possibly leading to conversion of non-Treg cells into Treg cells in women. On the other hand, stimulation of Treg and non-Treg cells from men with

DHT did not cause any change in the acetylation status of histone 4 within the *Foxp3* locus, thus preventing gene activation. These results indicate that the regulation of *Foxp3* expression by AR shows a gender-specific effect in T-cells. It seems that female T-cells obtained from a low-androgen environment are better ex vivo responders to androgen stimulation than male cells exposed to higher serum concentrations of testosterone.

Our data, together with other studies, indicate that high levels of testosterone seem to “lock” male T-cells by epigenetic mechanisms in a state of immune homeostasis. Conversely, the responsiveness of female T-cells to transform into Treg cells by variation of androgen levels may provide a mechanism to control excessive and putatively damaging immune responses in order to prevent immunopathology.

Taken together, our results provide novel evidence for a functional role of androgens in the generation of Treg cells and a molecular mechanism of *Foxp3* activation through androgen-mediated binding of AR to the *Foxp3* locus. This novel function of androgens in the immune response is not only important in male reproductive dysfunction such as autoimmune orchitis but could have much broader implications for understanding the pathophysiology of autoimmune diseases in general.

MATERIALS AND METHODS

T-cell isolation

PBMCs were isolated from buffy coats or fresh blood by density-gradient centrifugation using Ficoll-Paque Plus (GE Healthcare, Uppsala, Sweden). Buffy coats and blood samples were obtained from randomly selected healthy volunteer male and female blood donors after their informed consent (approved by the Ethics Committee of Giessen University, file number 05/00). For the treatment of Treg cells with DHT (Figure 1), blood samples were divided into male (age 20–35 and >60 yr) and female (age 20–35 and >50 yr) age-matched subgroups. Oral contraceptives were used by 50% of female donors, and there was no known medication and history of autoimmune disease of the donors. For ChIP experiments (interaction studies and epigenetic changes; Figures 3–5), Treg and T-cells were obtained from young (mean 26.3 ± 0.8 yr, *n* = 5) and older (mean 49.7 ± 1.3 yr, *n* = 4) women and young (mean 30.2 ± 2 yr, *n* = 5) and older (mean 47 ± 0.5 yr, *n* = 3) men. T-cells were purified from PBMCs using the human Pan T Cell Isolation Kit (influence of DHT on Treg cell differentiation) and human CD4⁺CD25⁺CD127^{dim/-} Regulatory T Cell Isolation Kit II (ChIP experiments). The purity of isolated Treg cells was >90%. For methylation analyses (Figure 7), CD4⁺CD25⁺ and CD4⁺CD25⁻ T-cells were isolated with the human

CD4⁺CD25⁺ Regulatory T Cell Isolation Kit. The purity of the CD4⁺CD25⁺ T-cell fractions was >98%. All Kits were obtained from Miltenyi Biotec (Bergisch Gladbach, Germany) and used according to the recommendations of the manufacturer. For methylation analyses, 4 × 10⁵ CD4⁺CD25⁺ T-cells were stimulated for 15 h with vehicle (ethanol) or 10 nM DHT.

Treatment of T-cells with DHT

To determine the effect of DHT on the differentiation of CD4⁺CD25⁺*Foxp3*⁺ T-cells, isolated T-cells from healthy donors were purified using the magnetic bead selection described (human Pan T Cell Isolation Kit). Isolated T-cells were stimulated every 24 h with DHT at doses ranging from 0 to 500 nM (Sigma-Aldrich, St. Louis, MO) in complete RPMI-1640 medium supplemented with 10% hormone-free serum (PAA, Cölbe, Germany) for 48 h at 37°C. Cells treated with vehicle (ethanol only) were used as control. Regulatory T-cells (Treg cells) were counted by flow cytometry.

Flow cytometric analyses

For flow cytometric analyses, the human Treg Detection Kit (CD4/CD25/*Foxp3*; Miltenyi Biotec) with the following antibodies was used: mouse anti-human CD4–fluorescein isothiocyanate (FITC), mouse anti-human CD25–phycoerythrin (PE), and mouse anti-human *Foxp3*–allophycocyanin (APC). Background staining was evaluated using appropriate isotype controls: immunoglobulin G1 (IgG1),κ-PE, mouse IgG1,κ-FITC, and mouse IgG1,κ-APC (BioLegend, London, United Kingdom). Data were collected over 50,000 events using a FACSCanto II flow cytometer (BD Biosciences, San Jose, CA) and analyzed with WinMDI version 2.8 and Flow Jo version X (TreeStar, Ashland, OR) software.

RNA isolation and qRT-PCR

Total RNA was extracted using the peqGold Total RNA Kit (PeqLab, Erlangen, Germany) and transcribed as described previously (Fijak *et al.*, 2011). RT-PCR was performed as described previously (Fijak *et al.*, 2011). The mRNA expression of all investigated genes was normalized based on the expression of the two housekeeping genes, *β-Actin* and *18SrRNA*. Primer sequences and amplicon sizes are shown in Table 3.

Cloning of AR and *Foxp3* gene constructs

Cloning of *Foxp3* gene fragments was performed with genomic DNA isolated from peripheral blood of a human male donor. Genomic DNA was isolated with the DNeasy Blood & Tissue Kit (Qiagen, Hilden, Germany) and used as a template to amplify *Foxp3*

Gene	Product length (base pairs)	Orientation	Primer sequence (5'–3')	Accession number
FOXP3	172	Forward	cggaccatcttctggatgag	NM_014009
		Reverse	ttgtcggatgatgccacag	
AR	198	Forward	ctactccggaccttacgggacatgcg	M34233
		Reverse	cacaggctactctgtttcccttcagcg	
<i>β-Actin</i>	90	Forward	ttccttctctgggcatggagt	NM 001101.3
		Reverse	ggcctgtaattggaatgagtc	
<i>18SrRNA</i>	146	Forward	ccaagatccaactacgagctt	X03205
		Forward	ccaagatccaactacgagctt	

TABLE 3: Sequences of forward and reverse primers used in qRT-PCR experiments and amplicon sizes.

gene fragments by PCR. The *Foxp3* promoter amplifcon was cloned into the *MluI/XhoI* restriction sites, the *Foxp3* fragment I (+277 to +2275), and fragment II (+2276 to +4399) into the *KpnI/MluI* restriction sites in front of the promoter fragment of the luciferase reporter vector pGL4-basic (Promega, Mannheim, Germany). For generation of deletion mutant $\Delta 698$ (+975 to +2275), fragment I was digested with *KpnI/SacI*. Ends were blunted with DNA-Polymerase I (Klenow) and ligated using T4 DNA Ligase (Promega). The fragments $\Delta 314$ (+591 to +2275) and $\Delta 523$ (+800 to +2275) were generated by PCR. Truncated parts of fragment I ($\Delta 314$ - and $\Delta 523$ -base pair mutants) were amplified by PCR with primers possessing *KpnI/SacI* restriction sites. Resulting PCR fragments were inserted into the *KpnI/SacI* sites of fragment I in pGL4 vector. The FL ΔF construct was generated by insertion of an additional *EcoRI* restriction site at position +1615 of the *Foxp3* gene with the GeneArt Site-Directed Mutagenesis System (Life Technologies, Darmstadt, Germany) according to the instructions of the manufacturer. The mutated construct was cut with *AflIII* and *EcoRI*, blunted with DNA-Polymerase I (Klenow) and ligated using T4 DNA Ligase (Promega). ARE C, D, and F mutations were introduced into *Foxp3* fragment I using the GeneArt Site-Directed Mutagenesis System (Life Technologies). The pcDNA3.1(+)-AR construct was generated by amplifying the human AR sequence by PCR using primers with *BamHI/XhoI* restriction sites and cloning into *BamHI/XhoI* site of the pcDNA3.1(+) vector. All constructs were verified by DNA sequencing (Microsynth, Göttingen, Germany). Primer sequences and cloning sites are shown in Supplemental Table S1.

Luciferase reporter gene assays

Luciferase assays were performed in HEK-293 cells seeded into 24-well plates in DMEM supplemented with 10% fetal bovine serum (FBS) and 0.5% of a penicillin-streptomycin mixture (all reagents from PAA). After transfections with FuGENE-HD reagent (Promega) and during DHT treatments, HEK-293 cells were cultured in DMEM supplemented with 10% charcoal-stripped FBS (PAA). Cells were transiently cotransfected with 0.25 μ g of *Foxp3* luciferase reporter constructs, 0.25 μ g of pcDNA3.1(+)-AR, and 0.025 μ g of pSV- β -Gal vector (Promega) as an internal control plasmid. Subsequently cells were stimulated with 0.5 nM DHT and cultured for 5 h. Supernatant of each sample were measured with the Luciferase Assay System Kit from Promega. The β -galactosidase results were used to normalize luciferase results for well-to-well variations.

Cross-linked chromatin immunoprecipitation assay

ChIP assays were performed with HEK-293 cells and freshly isolated human Treg cells using the human CD4⁺CD25⁺CD127^{dim/-} Regulatory T Cell Isolation Kit II (Miltenyi Biotec). HEK-293 cells were transiently cotransfected with either the *Foxp3* promoter or fragment I constructs/mutants together with the pcDNA3.1(+)-AR expression plasmid and treated with 0.5 nM DHT for 5 h. Cells were fixed with 1% formaldehyde (final concentration) for 10 min at room temperature, and cross-linking was stopped by adding 125 mM glycine (final concentration) for 5 min at room temperature. Washed cells were lysed in a solution consisting of 50 mM 4-(2-hydroxyethyl)-1-piperazineethanesulfonic acid-KOH (pH 7.5), 140 mM NaCl, 1 mM EDTA, 1% Triton X-100, 0.1% sodium deoxycholate, and 0.1% SDS supplemented with a protease inhibitor cocktail (Roche, Grenzach-Wyhlen, Germany) for 10 min while rotating at 4°C. Genomic DNA was sonicated to a mean size of ~500–700 base pairs. After removal of insoluble material by centrifugation, 10% of sonicated chromatin was saved for each sample to determine the input chromatin amount, and a 25- μ g amount was diluted fourfold in 50 mM Tris-HCl (pH 8.0), 150 mM NaCl, 2 mM EDTA, 1% IGEPAL CA-630, 0.5% sodium deoxycholate, 0.1% SDS, and protease inhibitor cocktail. Immunoprecipitation was performed using ChIP-grade rabbit anti-human AR antibody (Santa Cruz Biotechnology, Santa Cruz, CA), rabbit anti-human acetyl histone H4 (Millipore, Billerica, MA), rabbit anti-human trimethyl histone H3K27 (H3K27me3; Abcam, Cambridge, United Kingdom), and control human IgG (Abcam) overnight while rotating at 4°C. Chromatin-antibody complexes were recovered by incubation with protein A Dynabeads (Life Technologies) for 2 h at 4°C. Precipitates were washed serially with 1 ml of cold wash buffer I (20 mM Tris-HCl, pH 8.0, 150 mM NaCl, 2 mM EDTA, 1% SDS, 1% Triton X-100), 1 ml of cold wash buffer II (20 mM Tris-HCl, pH 8.0, 500 mM NaCl, 2 mM EDTA, 0.1% SDS, 1% Triton X-100), and 1 ml of cold wash buffer III (10 mM Tris-HCl, pH 8.0, 1 mM NaCl, 250 mM LiCl, 1% IGEPAL CA-630, 1% sodium deoxycholate) and once with 1 ml of cold TE-buffer (1 mM EDTA, 10 mM Tris-HCl, pH 8.0). Chromatin samples were dissociated from the beads twice with 100 μ l of 1% SDS and 100 mM NaHCO₃ each for 30 min at room temperature with constant agitation. Cross-linking was reversed by incubation with 500 mM NaCl at 65°C overnight. RNA and proteins were removed with 0.2 mg/ml RNaseA for 30 min at 37°C and 0.2 mg/ml proteinase K for 4 h at 56°C. DNA was purified with a PCR Purification Kit (PeqLab) and dissolved in 100 μ l of H₂O. DNA products were analyzed by qRT-PCR. Human Treg cells isolated from buffy

FOX P3 fragment	Region	Primer sequence (5'–3') forward	Primer sequence (5'–3') reverse
Promoter	A (–512 to –261)	catttccatccacacatagagct	ctgaaaatatgatttcttcccctcac
Promoter	B (–329 to +16)	tcatgagccctattatctcattgata	aaggatcagcctggctgtgggaaac
Fragment I	C (+738 to +897)	agcatcagttctgttcacctaagtagca	tccacacagctaaactacggttgacaatg
Fragment I	D (+898 to +1041)	cctaccaggactgcatgtgtgtgac	ataactaatgctaactctctgtgagc
Fragment I	E (+1047 to +1217)	taaccaaattagaatcatgctatatattg	caacaatcgccacttgtaaatcaatca
Fragment I	F (+1325 to +1649)	atgaccctctctgctaattctcctt	atatgtaatggctgatgaaagggttaat
Fragment I	G (+1531 to +1838)	tggtgtttttgtgatgcttatgatggttt	atggaggatggagaggggttaagtgcctggct
Fragment II	H (+2324 to +2512)	tctccatgtgggtccatgtccaagctt	gctggtcaactgatgctgctgaaa
Fragment II	I (+2485 to +2685)	atttcaggcagcatcagttgaaccagc	ggactggctgagagataggggatacatag
Fragment II	J (+3195 to +3403)	gattgtggggccctctagagagtctg	agccagcctcctagggctcagctcc
Fragment II	K (+3827 to +4015)	gaacgaaacctgtgggtgggtatctgc	gaatgggggatgtttctgggacacagatt

TABLE 4: Oligonucleotide primer sequences used for ChIP assays.

coats as described were used for the analysis of the AR-Foxp3 gene interaction and chromatin modifications. We treated 1×10^6 Treg cells with 10 mM DHT and performed ChIPs as described for transfected HEK-293 cells. Cells were lysed in 400 μ l of lysis buffer, immunoprecipitated with the same antibodies listed, and recovered by incubation with 20 μ l of protein A Dynabeads. DNA was purified with a PCR Purification Kit and dissolved in 50 μ l of H₂O.

To validate the ChIP assays, qRT-PCRs using an I-cycler iQ5 detection system were performed (Bio-Rad, Munich, Germany). Primer sequences of analyzed amplicons are shown in Table 4.

To see the enrichment of the immunoprecipitated sample compared with input material, the following calculation was made: $\Delta Ct = Ct(\text{input}) - Ct(\text{immunoprecipitated sample})$ and percentage total = $2\Delta Ct \times 10$ (when taking 10% of input chromatin).

Analysis of Foxp3 DNA methylation

Human T-cells (CD4⁺CD25⁻ and CD4⁺CD25⁺) were isolated using the human CD4⁺CD25⁺ Regulatory T Cell Isolation Kit (Miltenyi Biotec). Genomic DNA isolated from human T-cell subpopulations was extracted, bisulfite converted, and purified using the EpiTect Fast DNA Bisulfite Kit (Qiagen) according to the recommendations of the manufacturer. For amplification of specific CpG regions with the Foxp3 gene, 20 ng of bisulfite-converted DNA was used as a template in a PCR set up with the PyroMark PCR Kit (Qiagen). Different subsets of amplification primer pairs (Supplemental Table S2) were used. Methylation of specific CpGs was assessed by pyrosequencing of PCR products with the PyroMark Q24 kit (Qiagen) according to the recommendations of the manufacturer. Sequencing primers for the different regions are indicated in Supplemental Table S3. COBRA was carried out using the same bisulfite-converted DNA-templates (60 ng) as described for pyrosequencing. The relevant COBRA primer pairs used in subsequent PCRs with GoTaq polymerase (Promega) are indicated in Supplemental Table S4. PCR products were digested with TaqI (Thermo Scientific, Schwerte, Germany) for 3.5 h at 65°C according to the recommendations of the manufacturer. Band intensities of undigested and digested PCR fragments were compared and quantified with Quantity One Basic software (Bio-Rad).

Statistical analysis

Results are expressed as mean \pm SEM. Comparisons between groups were assessed using the nonpaired Student's *t* test or the Wilcoxon–Mann–Whitney test, depending on the distribution of data. The one-way analysis of variance (ANOVA) was accompanied by the Bonferroni test to calculate confidence intervals. $p < 0.05$ was considered statistically significant.

Additional materials and methods

Additional experimental protocols are presented in the supplemental material.

ACKNOWLEDGMENTS

We thank Aria Baniahmad and Ulrich Steinhoff for expert consulting and valuable suggestions and Klaus Steger for providing the pyrosequencer. This work was supported by a grant of the State of Hessen program Landes-Offensive zur Entwicklung Wissenschaftlich-ökonomischer Exzellenz–Männliche Infertilität bei Infektion und Entzündung.

REFERENCES

Akhtar A, Becker PB (2000). Activation of transcription through histone H4 acetylation by MOF, an acetyltransferase essential for dosage compensation in *Drosophila*. *Mol Cell* 5, 367–375.

- Allfrey VG, Faulkner R, Mirsky AE (1964). Acetylation and methylation of histones and their possible role in the regulation of RNA synthesis. *Proc Natl Acad Sci USA* 51, 786–794.
- Arruvito L, Sanz M, Banham AH, Fainboim L (2007). Expansion of CD4+CD25+ and FOXP3+ regulatory T cells during the follicular phase of the menstrual cycle: implications for human reproduction. *J Immunol* 178, 2572–2578.
- Bebo BF Jr, Zelinka-Vincent E, Adamus G, Amundson D, Vandenberg AA, Offner H (1998). Gonadal hormones influence the immune response to PLP 139–151 and the clinical course of relapsing experimental autoimmune encephalomyelitis. *J Neuroimmunol* 84, 122–130.
- Burger HG (2002). Androgen production in women. *Fertil Steril* 77(Suppl 4), S3–S5.
- Chen W, Jin W, Hardegen N, Lei KJ, Li L, Marinos N, McGrady G, Wahl SM (2003). Conversion of peripheral CD4+CD25- naive T cells to CD4+CD25+ regulatory T cells by TGF-beta induction of transcription factor Foxp3. *J Exp Med* 198, 1875–1886.
- Chmela R, Buchanan G, Need EF, Tilley W, Greenberg NM (2007). Androgen receptor coregulators and their involvement in the development and progression of prostate cancer. *Int J Cancer* 120, 719–733.
- Fijak M, Schneider E, Klug J, Bhushan S, Hackstein H, Schuler G, Wygrecka M, Gromoll J, Meinhardt A (2011). Testosterone replacement effectively inhibits the development of experimental autoimmune orchitis in rats: evidence for a direct role of testosterone on regulatory T cell expansion. *J Immunol* 186, 5162–5172.
- Fitzpatrick F, Lepault F, Homo-Delarche F, Bach JF, Dardenne M (1991). Influence of castration, alone or combined with thymectomy, on the development of diabetes in the nonobese diabetic mouse. *Endocrinology* 129, 1382–1390.
- Floess S, Freyer J, Siewert C, Baron U, Olek S, Polansky J, Schlawe K, Chang HD, Bopp T, Schmitt E, et al. (2007). Epigenetic control of the foxp3 locus in regulatory T cells. *PLoS Biol* 5, e38.
- Fontenot JD, Rasmussen JP, Gavin MA, Rudensky AY (2005). A function for interleukin 2 in Foxp3-expressing regulatory T cells. *Nat Immunol* 6, 1142–1151.
- Goebelsmann U, Arce JJ, Thorneycroft IH, Mishell DR Jr (1974). Serum testosterone concentrations in women throughout the menstrual cycle and following HCG administration. *Am J Obstet Gynecol* 119, 445–452.
- Hedman M, Nilsson E, de la Torre B (1989). Low sulpho-conjugated steroid hormone levels in systemic lupus erythematosus (SLE). *Clin Exp Rheumatol* 7, 583–588.
- Heinlein CA, Chang C (2002). Androgen receptor (AR) coregulators: an overview. *Endocr Rev* 23, 175–200.
- Hori S, Nomura T, Sakaguchi S (2003). Control of regulatory T cell development by the transcription factor Foxp3. *Science* 299, 1057–1061.
- Hu S, Yao G, Guan X, Ni Z, Ma W, Wilson EM, French FS, Liu Q, Zhang Y (2010). Research resource: genome-wide mapping of in vivo androgen receptor binding sites in mouse epididymis. *Mol Endocrinol* 24, 2392–2405.
- Huehn J, Polansky JK, Hamann A (2009). Epigenetic control of FOXP3 expression: the key to a stable regulatory T-cell lineage? *Nat Rev Immunol* 9, 83–89.
- Kim HP, Leonard WJ (2007). CREB/ATF-dependent T cell receptor-induced FoxP3 gene expression: a role for DNA methylation. *J Exp Med* 204, 1543–1551.
- Klein SL (2012). Immune cells have sex and so should journal articles. *Endocrinology* 153, 2544–2550.
- Lal G, Bromberg JS (2009). Epigenetic mechanisms of regulation of Foxp3 expression. *Blood* 114, 3727–3735.
- Lee JH, Lydon JP, Kim CH (2012). Progesterone suppresses the mTOR pathway and promotes generation of induced regulatory T cells with increased stability. *Eur J Immunol* 42, 2683–2696.
- Leposavić G, Perišić M, Kosec D, Arsenović-Ranin N, Radojević K, Stojić-Vukanić Z, Pilipović I (2009). Neonatal testosterone imprinting affects thymus development and leads to phenotypic rejuvenation and masculinization of the peripheral blood T-cell compartment in adult female rats. *Brain Behav Immun* 23, 294–304.
- Mantalaris A, Panoskaltsis N, Sakai Y, Bourne P, Chang C, Messing EM, Wu JH (2001). Localization of androgen receptor expression in human bone marrow. *J Pathol* 193, 361–366.
- Oertelt-Prigione S (2012). The influence of sex and gender on the immune response. *Autoimmun Rev* 11, A479–A485.
- Ogawa C, Tone Y, Tsuda M, Peter C, Waldmann H, Tone M (2014). TGF-beta-mediated Foxp3 gene expression is cooperatively regulated by Stat5, Creb, and AP-1 through CNS2. *J Immunol* 192, 475–483.

- Ohkura N, Kitagawa Y, Sakaguchi S (2013). Development and maintenance of regulatory T cells. *Immunity* 38, 414–423.
- Peters AH, Kubicek S, Mechtler K, O'Sullivan RJ, Derijck AA, Perez-Burgos L, Kohlmaier A, Opravil S, Tachibana M, Shinkai Y, et al. (2003). Partitioning and plasticity of repressive histone methylation states in mammalian chromatin. *Mol Cell* 12, 1577–1589.
- Piccirillo CA, Shevach EM (2001). Cutting edge: control of CD8+ T cell activation by CD4+CD25+ immunoregulatory cells. *J Immunol* 167, 1137–1140.
- Polanczyk MJ, Hopke C, Huan J, Vandenbark AA, Offner H (2005). Enhanced FoxP3 expression and Treg cell function in pregnant and estrogen-treated mice. *J Neuroimmunol* 170, 85–92.
- Rothman MS, Carlson NE, Xu M, Wang C, Swerdloff R, Lee P, Goh VH, Ridgway EC, Wierman ME (2011). Reexamination of testosterone, dihydrotestosterone, estradiol and estrone levels across the menstrual cycle and in postmenopausal women measured by liquid chromatography-tandem mass spectrometry. *Steroids* 76, 177–182.
- Rudensky AY (2011). Regulatory T cells and Foxp3. *Immunol Rev* 241, 260–268.
- Sakaguchi S, Yamaguchi T, Nomura T, Ono M (2008). Regulatory T cells and immune tolerance. *Cell* 133, 775–787.
- Schumacher A, Brachwitz N, Sohr S, Engeland K, Langwisch S, Dolaptchieva M, Alexander T, Taran A, Malfertheiner SF, Costa SD, et al. (2009). Human chorionic gonadotropin attracts regulatory T cells into the fetal-maternal interface during early human pregnancy. *J Immunol* 182, 5488–5497.
- Sekiya T, Kashiwagi I, Inoue N, Morita R, Hori S, Waldmann H, Rudensky AY, Ichinose H, Metzger D, Chambon P, Yoshimura A (2011). The nuclear orphan receptor Nr4a2 induces Foxp3 and regulates differentiation of CD4+ T cells. *Nat Commun* 2, 269.
- Stafford L, Bleasel J, Giles A, Handelsman D (2000). Androgen deficiency and bone mineral density in men with rheumatoid arthritis. *J Rheumatol* 27, 2786–2790.
- Struhl K (1998). Histone acetylation and transcriptional regulatory mechanisms. *Genes Dev* 12, 599–606.
- Tai P, Wang J, Jin H, Song X, Yan J, Kang Y, Zhao L, An X, Du X, Chen X, et al. (2008). Induction of regulatory T cells by physiological level estrogen. *J Cell Physiol* 214, 456–464.
- Thornton AM, Shevach EM (1998). CD4+CD25+ immunoregulatory T cells suppress polyclonal T cell activation in vitro by inhibiting interleukin 2 production. *J Exp Med* 188, 287–296.
- Tone Y, Furuuchi K, Kojima Y, Tykocinski ML, Greene MI, Tone M (2008). Smad3 and NFAT cooperate to induce Foxp3 expression through its enhancer. *Nat Immunol* 9, 194–202.
- Vakoc CR, Mandat SA, Olenchock BA, Blobel GA (2005). Histone H3 lysine 9 methylation and HP1gamma are associated with transcription elongation through mammalian chromatin. *Mol Cell* 19, 381–391.
- Vakoc CR, Sachdeva MM, Wang H, Blobel GA (2006). Profile of histone lysine methylation across transcribed mammalian chromatin. *Mol Cell Biol* 26, 9185–9195.
- Viselli SM, Reese KR, Fan J, Kovacs WJ, Olsen NJ (1997). Androgens alter B cell development in normal male mice. *Cell Immunol* 182, 99–104.
- Zhou J, Wang Z, Zhao X, Wang J, Sun H, Hu Y (2012). An increase of Treg cells in the peripheral blood is associated with a better in vitro fertilization treatment outcome. *Am J Reprod Immunol* 68, 100–106.